CHEMPHYSCHEM

DOI: 10.1002/cphc.200800703

How Does a Membrane Protein Achieve a Vectorial Proton Transfer Via Water Molecules?

Steffen Wolf, Erik Freier, and Klaus Gerwert*[a]

We present a detailed mechanism for the proton transfer from a protein-bound protonated water cluster to the bulk water directed by protein side chains in the membrane protein bacteriorhodopsin. We use a combined approach of time-resolved Fourier transform infrared spectroscopy, molecular dynamics simulations, and X-ray structure analysis to elucidate the functional role of a hydrogen bond between Ser193 and Glu204. These two residues seal the internal protonated water cluster from the bulk water and the protein surface. During the photocycle of bacteriorhodopsin, a transient protonation of Glu204 leads to a breaking of this hydrogen bond. This breaking opens the gate to the extracellular bulk water, leading to a subsequent proton release from the protonated water cluster. We show in detail how the protein achieves vectorial proton transfer via protonated water clusters in contrast to random proton transfer in liquid water.

Introduction

How protons migrate in water has been a central question in physical chemistry for more than two centuries, ever since Grotthuss[1] proposed the transfer along water molecule chains and Eigen[2] identified fast proton-transfer reactions in larger protonated water clusters ($H_9O_4^+$). Proton transfer is random in water. However, in living cells a vectorial proton transfer occurs via photosynthesis or in cell respiration. These two elementary processes in bioenergetics provide a proton gradient, the force for driving ATP (adenosine triphosphate) synthesis, is the fuel for living cells.[3]

High resolution crystal structures of crucial membrane proteins involved in these two elementary bioenergetic processes, the photosynthetic proteins, and the cytrochrome c-oxydase reveal internal protein-bound water molecules. Recent research proposes that these protein-bound water molecules are actively involved in the vectorial proton transfer.[4–8] However, it is not yet understood in detail how these proteins achieve a vectorial proton transfer within the proteins to create a proton gradient in contrast to random proton transfer in water.

An excellent model system to study the role of internal water molecules in proton transfer is the light-driven proton pump bacteriorhodopsin (bR), a well characterized heptahelical transmembrane retinal protein.[5,9] Upon light excitation the retinal chromophore undergoes an *all-trans* to *13-cis* isomerization. The retinal is covalently bound via a protonated Schiff base to the Lys216 of the opsin. The isomerization drives a photocycle with the intermediates K, L, M, N, and O, in order of their appearance. The photocycle is accompanied by a proton transfer from the intracellular to extracellular medium. In this way, a proton gradient is created. High resolution X-ray structural analysis of bR in its ground state at 100 K[10,11] identified several internal protein-bound water molecules, especially on the proton release pathway. Time-resolved Fourier transform infrared (FTIR)[5,9,12] and complementary molecular dynamics (MD) studies[13,14] explain the detailed proton transfer via these water molecules on the proton release site from the internal central proton binding site, the protonated Schiff base, to the protein surface (see Figure 1 for a detailed description). It involves a strong hydrogen bounded water, a dangling water close to the central proton binding site and a protonated water complex $H(H_2O)_4^+$ as the proton release group (see Figure 1).

The question that remains is: how does this membrane protein achieve the directionality of the proton transfer via these protein-bound water molecules? To answer this question, we used a combined approach of protein crystallography, time-resolved FTIR spectroscopy, and MD simulations. We demonstrate an electromechanical switch on the proton exit site of bacteriorhodopsin. Upon proton transfer from the protonated Schiff base to its counter ion Asp85[5,9], a hydrogen bond between Ser193 and Glu204 opens selectively. This leads to an opening of the Ser193 and Glu204 gate and a subsequent proton release to the bulk solvent, resulting in the net transfer of one proton across the membrane.

Results and Discussion

FTIR Measurements I: Transient Protonation of Glu204 at pH 5

Figures 2A and B show the time-resolved absorbance changes of the retinal C14–C15 stretching vibration at 1186 cm^{-1} in

[a] *S. Wolf,[+] E. Freier,[+] Prof. Dr. K. Gerwert*
Department of Biophysics
ND 04 North, Ruhr-University BochumD-44780 Bochum (Germany)
Fax: (+49) 234 32 14626
E-mail: gerwert@bph.rub.de

[+] *These authors contributed equally to this work.*

Supporting information for this article is available on the WWW under http://dx.doi.org/10.1002/cphc.200800703.

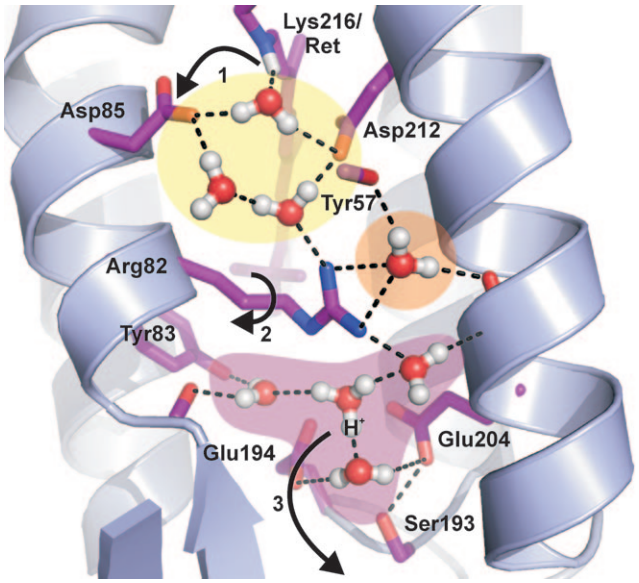

Figure 1. Proton release mechanism in bR in the L–M transition. Important residues shown as sticks, internal waters as balls and sticks, water pentamer with dangling water highlighted in yellow, water molecule between Tyr57 and Arg82 in orange, protonated Eigen cluster in purple. Upon light excitation of the ground state molecule (BR), the retinal chromophore changes its conformation from *all-trans* to *13-cis*, forming the L intermediate. This change triggers the transfer of the proton from the protonated Schiff base to Asp85 (1), which leads to a breakdown of the water pentamer structure. It is followed by a downward movement of Arg82 (2). This conformational change affects the positions of the waters of the Eigen ion, which leads to the release of the proton to the bulk solvent (3).

wild type (WT) bR at pH 5 and 7. It reflects the deprotonation of the protonated Schiff base by $k_{L\text{-}M}$ in the L to M transition, the reprotonation of the Schiff base in the M to N transition by $k_{L\text{-}M}$ and the reisomerisation to all-trans by $k_{O\text{-}BR}$. In the wild type at pH 5 (B), less M intermediate is accumulated in comparison to the wild type at pH 7 (A).

Figures 2C and D show the respective time-resolved continuum band absorbance changes[9] between 1900–1800 cm^{-1} in wild type bR at pH 5 and 7. It indicates the deprotonation of the protonated water cluster in the L to M transition by $k_{L\text{-}M}$. The molecular meaning of the second rate $k_{M\text{-}N}$ is not yet fully understood. In comparison to the wild type at pH 7, the amplitude of the $k_{L\text{-}M}$ rate at pH 5 is also reduced as compared to the rate $k_{M\text{-}N}$. It was shown that at pH 5, the proton release is delayed.[9,15,16] We therefore conclude that the reduction of the pH from 7 to 5 slows down the proton release, which in turn hinders the accumulation of M intermediate.

Figure 3A shows the M intermediate spectra of WT bR at pH 5 and 7 and the Ser193A mutant at pH 7 in the regime between 1780 and 1700 cm^{-1}, indicating protonation changes of Asp and Glu. The wild type shows deviations between pH 7 and pH 5 (marked in light grey). Surprisingly, the S193A mutant at pH 7 shows the same spectral feature as the wild type at pH 5 (highlighted in light grey in Figure 3A). This regime was assigned to the protonation changes of Glu194 and 204.[9] As can be seen in Figure 3B, the appearance of the band at 1720 to 1707 cm^{-1} in WT at pH 5 (shown in black) takes place with the same time constant (k_{M-N}) as the first rate of the continuum absorbance decrease (shown in dashed grey lines). From this result it can be concluded that in wild type protein at pH 5, a change in the protonation state of the glutamates 194 and 204 takes place. This might explain the delayed proton release at pH 5, which is delayed from L to M at pH 7 to the M to N/O transition at pH 5.[9,15] The WT at pH 5 was chosen to study the features of the late proton release, which can be observed at a pH lower than pH 6.[16] Interestingly, mutations of S193 induce a similar effect as increasing of the proton concentration in the bulk solvent to a pH of 5.

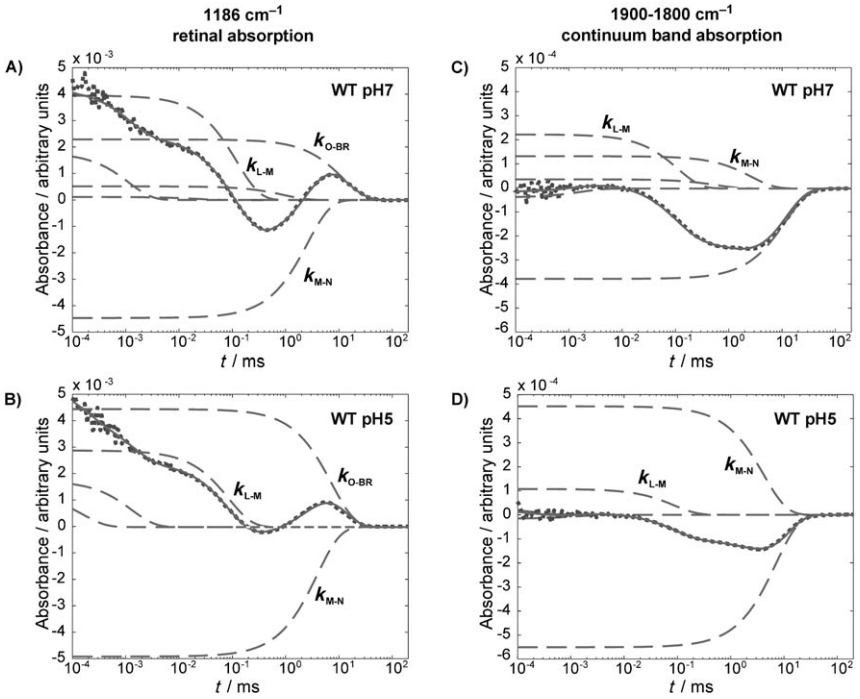

Figure 2. Time-resolved retinal absorbance at 1186 cm^{-1} for WT bR at pH 7 (A) and pH 5 (B). The photocycle is intact for the wild type at pH 5 and at pH 7, with a smaller accumulation of the M intermediate at pH 5. C and D: Time-resolved continuum band absorbance at 1900–1800 cm^{-1}. While WT bR shows a higher intensity of the first rate of the continuum absorption ($k_{L\text{-}M}$) than the second rate ($k_{M\text{-}N}$) during the photocycle, it is lower in intensity than $k_{M\text{-}N}$ at pH 5. In all spectra (••••): data, (——): resulting global fits, and (----): fit components.

MD Simulations I: S193/Glu204 as Gatekeepers of the Proton Release Group

From the spectral characterisation mentioned above, it can be derived that Ser193 and Glu204 play an important role in the

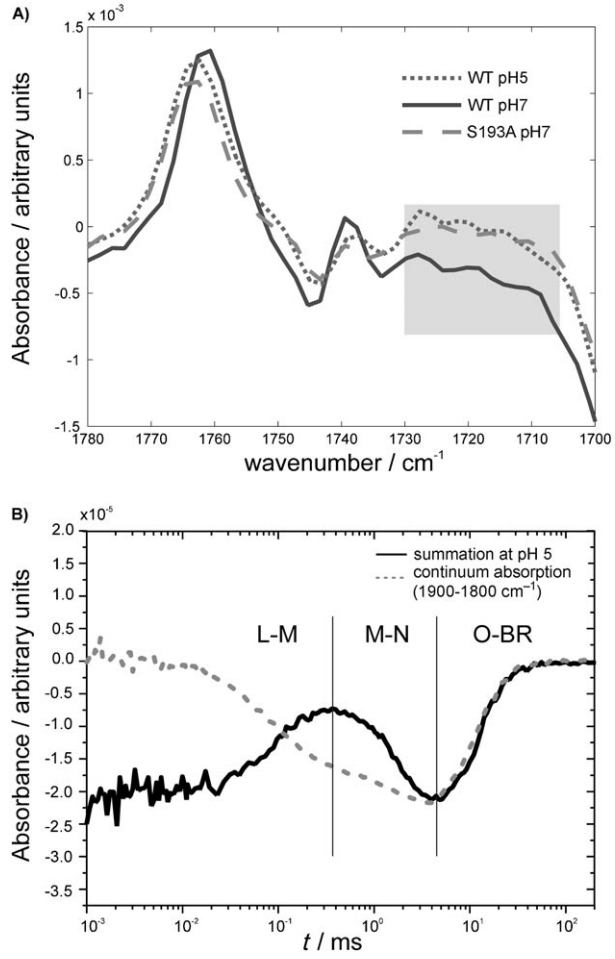

Figure 3. A) Spectra of the M intermediates of bR in the regime from 1780 to 1700 cm^{-1}. In the regime between 1730 and 1707 cm^{-1}, changes (highlighted in light grey) from the wild type at pH 7 can be observed which are the same for wild type at pH 5 and the S193A mutant at pH 7. The apparent offset in WT at pH 7 is due to the reduced continuum absorbance in WT at pH 5 (see Figure 2) and the S193A mutant.[9] B) Time course of the band in the 1720 to 1707 cm^{-1} regime of the WT protein at pH 5. The band first appear in the L to M transition, and then vanishes in the M to N transition. The appearance between 1720 and 1707 cm^{-1} takes place at the same time as the first rate of the continuum absorbance, indicating an involvement in the proton release.

proton release. We therefore carried out MD simulations to understand their function. The dynamics of water positions at the release site are analysed by means of time-dependent water residences per volume unit (hereon referred to as water densities following the terminology from Kandt et al.[14]).

As can be seen in Figure 4, Ser193 is the protein residue that seals the protonated water cluster from the extracellular solvent by forming a hydrogen bond to Glu204 (A). This hydrogen bond is stable during the whole period of sampling (B). It shields the protonated water cluster from the surrounding solvent. This hydrogen bond might act as a gatekeeper for water. Actually, in our earlier MD simulation, the protonated water cluster was roughly modelled by a protonation of Glu204.[14] The resulting simulation showed an opening of the proton exit site between Ser193 and Glu204. Here we improved our simulation and placed the proton explicitly into the internal water cluster as indicated in Figure 1 in form of a hydronium ion. Consequently we observed a different behaviour.

Hence, we can conclude from the MD simulations that the hydrogen bond observed between Ser193 and Glu204 is sensitive to the charge state on Glu204. A protonation of the carboxyl oxygens of Glu204 will lead to a rupture of the hydrogen bond and to an opening of the proton release group to the bulk water.

Evidence for the Ser193/Glu204 Gate in X-Ray Structure Analysis

Figure 5 shows crystal structures of ground state and photocycle intermediates of bR, which further support the functional role of the Ser193/Glu204 hydrogen bond. In the wild type ground state crystal structure (WT, PDB ID 1C3W, 1.55 Å resolution)[11] the side chain oxygen atoms of Ser193 and Glu204 are at a distance of 2.6 Å, and the Connolly surface of the protonated water cluster and the extracellular protein surface are separated by 4.1 Å. The distance between Ser193 and Glu204 is increased to 2.9 Å in the M_1 structure measured at 100 K (WT, PDB ID 1M0M, 1.62 Å resolution).[10] It shows an opening to the

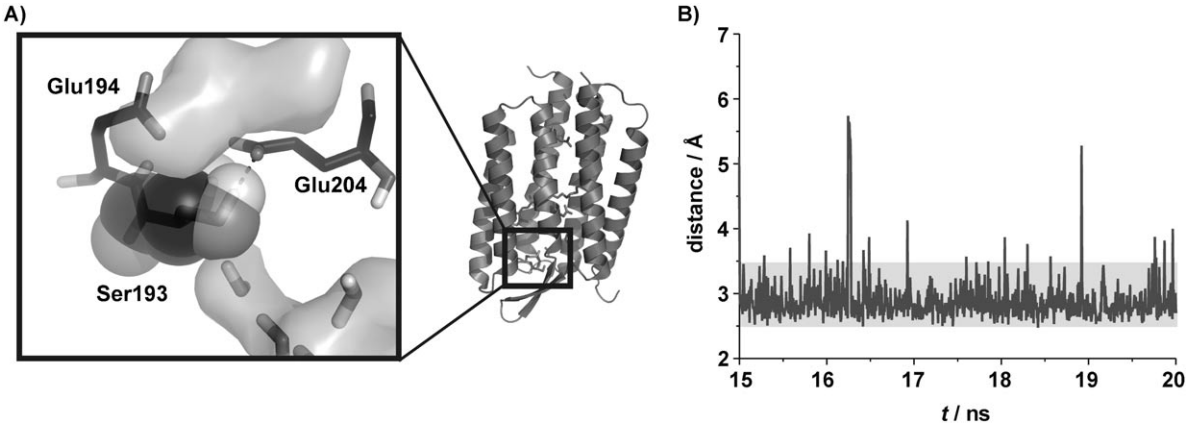

Figure 4. A) Water densities at the extracellular surface of the proton exit site during the final 5 ns of simulation in WT protein at pH 7. Protein in black, water densities in grey, Ser193 highlighted as transparent spheres. In the WT protein, the extracellular bulk water can enter the protein up until Ser193. B) Minimal distance of Ser193 and Glu204 head groups. During the whole course of sampling, Ser193 forms a hydrogen bond to Glu204 (hydrogen bond distances highlighted in light grey) and thereby a barrier to the protonated water cluster.

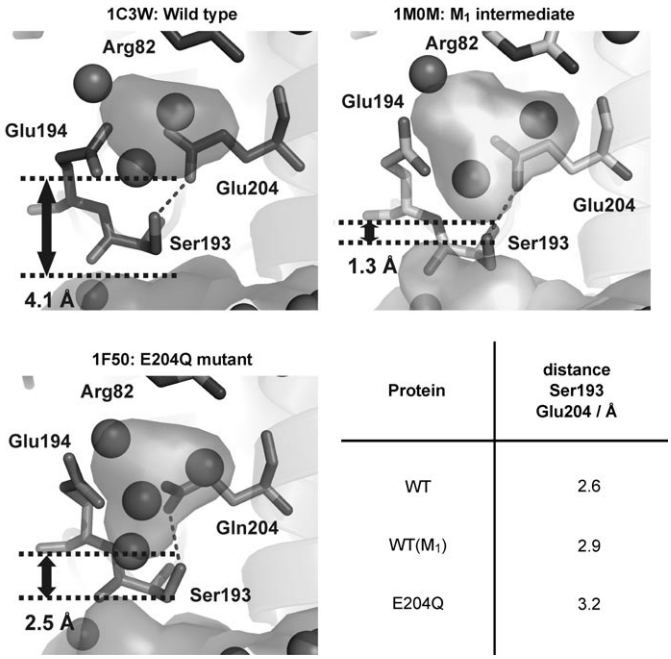

Protein	distance Ser193 Glu204 / Å
WT	2.6
WT(M_1)	2.9
E204Q	3.2

Figure 5. The Ser193/Glu204 hydrogen bond and Connolly surfaces of the proton exit site in bR crystal structures. Arg82, Ser193, Glu194, and Glx204 shown as sticks. Water molecule positions shown as spheres. Top left: Ground state (WT, PDB ID 1C3W). Top right: M_1 intermediate (WT, PDB ID 1M0M). Bottom left: Mimic for protonated Glu204 (E204Q mutant, PDB ID 1F50). In the ground state, the hydrogen bond partners are at a distance of 2.6 Å. The proton exit site and the extracellular surface are well separated by a distance of 4.1 Å. In the M_1 state, the hydrogen bond is lengthened to 2.9 Å. The Connolly surfaces of proton exit and extracellular site are close enough to allow direct contact between the water cluster and bulk solvent (distance of 1.3 Å). In the E204Q structure, the distance shows a further increase to 3.2 Å. The Connolly surfaces are close enough to allow direct water contact between water cluster and bulk solvent (distance of 2.5 Å). An additional water molecule is found between internal and external surface, which establishes a hydrogen bond connection between water cluster and bulk water.

bulk water (distance of Connolly surfaces of 1.3 Å) and a weakening of the hydrogen bond by increasing its length to 2.9 A. The structure of the E204Q mutant (PDB ID 1F50, 1.7 Å resolution)[17] shows an even greater increase in Ser193/Glu204 distance (3.2 Å), and is open to the bulk solvent by placing a novel water molecule between the Connolly surface of the water cluster and the extracellular protein surface. This water molecule forms a connection between the protein internal water cluster and bulk solvent.

This and the findings of our *in silico* investigations imply that the opening of the proton exit site is only dependent on the protonation state of Glu204, which is coupled to the protonation state of Schiff base counter ion Asp85 via Arg82 in WT bR.[18] As Gln204 is an isoelectric mimic for a permanently protonated Glu204, the mutant protein is already open to the bulk water in the ground state. As a result, the opening mechanism is decoupled from the protonation state of Asp85 in this mutant bR.

MD Simulations II: Influencing the Proton Exit Pathway Via *in silico* Mutations

As the S193A mutant shows the same behaviour as the WT protein at pH 5, we wanted to elucidate the effect of this mutation onto the bR structure, and predict further mutants which might influence the proton exit mechanism. For this purpose, we chose a S193C mutation. Such a mutation would retain the size of the Ser193 side chain, while reducing the side chain dipole moment and therefore the strength of any hydrogen bond formed by it. As crystal structures of Ser193 mutants are missing, we focussed on *in silico* mutants in our investigation.

Figure 6 shows the effect of the proposed S193A and S193C mutants. In the S193A mutant, the water channel leading to the proton exit site collapsed, creating a hydrophobic barrier between the protonated water cluster and the extracellular solvent. In contrast, in the S193C mutant, the extracellular solvent can enter into the protein and forms direct contact with Glu204. Cys193 temporarily forms a hydrogen bond to Glu204, but most of the time is too distant from Glu204 to form such a bond. Its side chain moves arbitrarily between the two water densities, forming a diffusion barrier (using the terminology of Kandt et al.[14]) for the intruding water. In both mutants, bulk water and the protonated water cluster are therefore separat-

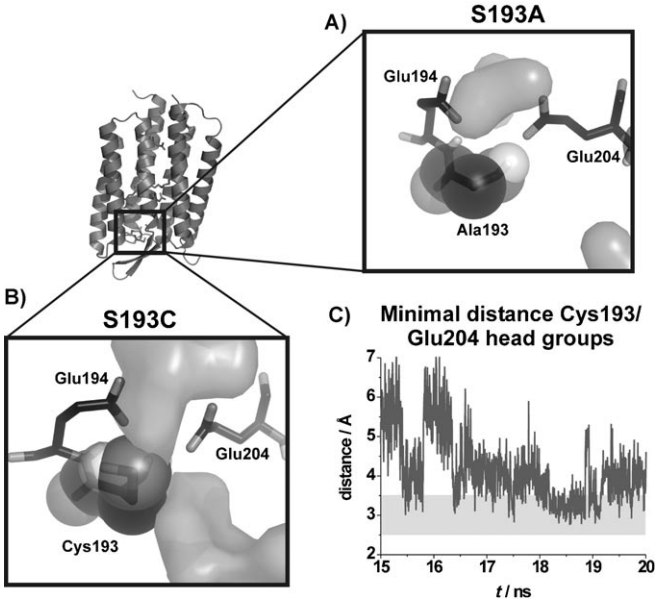

Figure 6. Water densities at the extracellular surface of the proton exit site during the final 5 ns of simulation. A) S193A mutant. Protein in black, water densities in grey, Ala193 highlighted as transparent spheres. In the S193A mutant, the bulk water entrance pathway to amino acid No. 193 has collapsed. B) S193C mutant. Protein in black, water densities in grey, Cys193 highlighted as transparent spheres. In the S193C mutant, bulk water can enter the protein up until Glu204. Cys193 places its flexible side chain directly between the water densities of extracellular water and the protonated water cluster, forming a diffusion barrier, but only temporarily a hydrogen bond to Glu204. C) Minimal distance of Cys193 and Glu204 head groups. During the whole course of sampling, Cys193 only temporarily forms a hydrogen bond to Glu204 (hydrogen bond distances highlighted in light grey) and is therefore disconnected from Glu204.

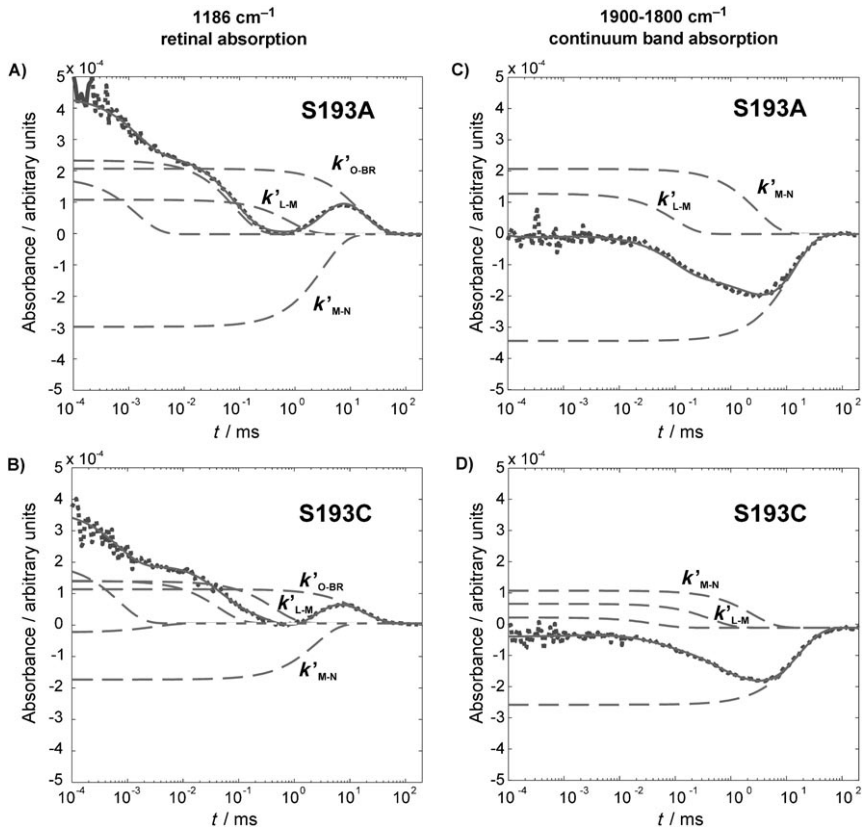

Figure 7. Time-resolved retinal absorption at 1186 cm^{-1} for bR mutants S193A (A) and S193C (B) at pH 7. The photocycle is intact for both mutants, with a smaller accumulation of the M intermediate. C) and D) Time-resolved continuum band absorption at 1900–1800 cm^{-1}. Both bR mutants shows a higher intensity of the second rate of the continuum absorption ($k'_{M\text{-}N}$) than the first rate ($k'_{L\text{-}M}$) during the photocycle, which is comparable to the results for WT bR at pH 5. In all spectra (•••••): data, (——): resulting global fits, and (-----): fit components.

ed by amino acid side chains, which are not connected to Glu204 and therefore form an additional barrier. The mutations are proposed to delay or inhibit the proton release like the WT at pH 5.

FTIR Measurements II: S193A and S193C Exhibit a Transient Protonation of Glu204

To verify our predictions from MD simulations, we carried out further FTIR measurements on S193C along with further analysis of S193A. Figures 7 A and B show the time-resolved absorbance changes of the retinal C14–C15 stretching vibration at 1186 cm^{-1} in S193A and S193C at pH 7. In both mutants, less M intermediate is accumulated as in WT protein at pH 5. The effect is, however, less pronounced in S193C than in S193A. Figures 7 C and D show the time-resolved continuum band absorbance[5] at 1900–1800 cm^{-1} in both mutants at pH 7. In both mutants, the intensity of $k'_{L\text{-}M}$ is less than the second rate $k'_{M\text{-}N}$ of the continuum absorption. It was shown that S193A, like WT protein at pH 5, exhibits a delayed proton release.[9,15]

Figure 8 A shows the behaviour of the 1720–1707 cm^{-1} regime in WT protein at pH 5 and 7 and the S193 A mutant at pH 7. It can clearly be seen that both WT at pH 5 and the S193A mutant at pH 7 exhibit the same spectral feature, accounting for a transient protonation of Glu204 that cannot be observed in the WT protein at pH 7. Furthermore, a comparison of WT bR, and the S193A and S193C mutants at pH 7 (Figure 8 B) shows that S193C exhibits the same spectral feature, although it is less prominent, possibly due to lesser band intensity in the spectrum and an overlap with continuum absorption. This indicates a transient protonation of glutamates 194 and/or 204 during the proton release in S193C as well, which confirms our prediction from MD simulations.

Model of a Directional Proton Release Mechanism

If we consider both the results from MD simulations and X-ray structural analysis, our FTIR measurements indicate that the hydrogen bond between Ser193 and Glu204 is an important gate for the proton release mechanism. The absence of this hydrogen bond leads to a major delay in the disappearance of the continuum absorbance change (see Figure 2) and thus the proton exit from bR.[5,9,12] Like WT bR, the S193C mutant exhibits a pathway for bulk water up to amino acid No. 193 in our *in silico* simulations, but the position of the cysteine side chain is not coupled to the charge state of Glu204. It seems that the hydrogen bond itself is a crucial structural feature to perform a controlled, fast and efficient exit of the proton upon the occurrence of the M intermediate.

Furthermore, our findings show that the hydrogen bond formation depends on the protonation state of Glu204. A deprotonated state favours a hydrogen bond, while a protonated Glu204 leads to a rupture of the bond. Upon a protonation of Glu204 and subsequent breaking of the bond to Ser193, the protonated water cluster becomes exposed to the extracellular solvent and the proton is therefore released to the bulk water. Mutations of Ser193 to Ala or Cys, as well as a rise in proton concentration in the bulk solvent, increase the barrier for the proton release. Therefore, in contrast to WT at pH 7, a transient protonation of glutamates 194 and/or 204, is observed in the FTIR measurements. The transient protonation in the WT is too short to be detected. At low temperature the lifetime, of the transient protonation might become long enough for detection via FTIR measurements. However, the proton release mechanism is changed at low temperature in comparison to room temperature, as described by Lórenz-Fonfría et al.,[19]

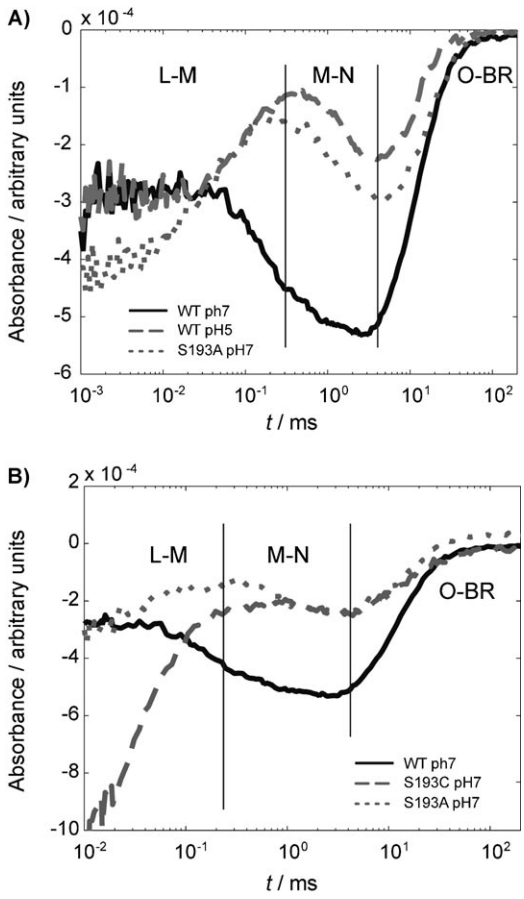

Figure 8. A) Time course of the band in the 1720 to 1707 cm^{-1} regime of WT protein at pH 5 and 7, and the S193A mutant at pH 7. While the WT bR at pH7 only shows continuum absorbance changes in this regime, WT bR at pH 5 and in the S193A mutant at pH 7 show an appearance of a band in the L to M transition, which then vanishes in the M to N transition. The appearance between 1720 and 1707 cm^{-1} takes place at the same time as the first rate of the continuum absorption, indicating an involvement in the proton release. B) Time course of the band in the 1720 to 1707 cm^{-1} regime of WT protein at pH 7 and the S193A and S193C mutant at pH 7. S193C exhibits the same spectral feature as WT bR at pH 5 and S193A, although it is less prominent, possibly due to a smaller band intensity in the spectrum and an overlap with continuum absorption.

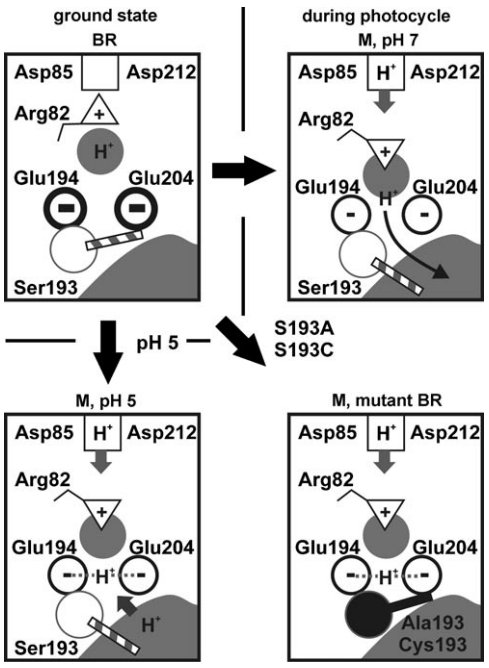

Figure 9. Hypothetical mechanism of the directional proton release and influence from pH and mutations of Ser193. The protonation of Asp85 upon formation of the M state induces a shift of Arg82. This affects the position of the proton in the exit site and pushes it towards glutamates 194 and 204. The proton quenches the negative charge of the glutamates, leading to a weakening/breaking of the hydrogen bond between Ser193 and Glu204. The exit site opens up to the extracellular bulk solvent and the proton leaves the protein. At pH 5, the difference in potential between Asp85 and the bulk solvent is not high enough to provide a fast proton exit. Instead, Arg82 pushes the proton onto the glutamates 194 and 204. Removal of the hydrogen bond between Ser193 and Glu204 by mutation of Ser193 increases the barrier effect of amino acid 193 between the protonated water cluster and bulk solvent. The proton is pushed onto the glutamates 194 and/or 204 in the S913 A or S193C mutants.

possibly due to a change of the proton location in the proton release group.

Based on these results, we present a hypothesis for a controlled release mechanism of the proton during the photocycle. It accounts for the vectoriality of the proton transfer and is summarised in Figure 9. In the ground state, Asp85 forms a salt bridge to Arg82. The protonated water cluster stabilizes the negative charges of Glu194 and Glu204. Ser193 forms a hydrogen bond to Glu204 and therefore closes the connection between extracellular solvent and the water cluster like a gate. Upon protonation of Asp85, its negative charge becomes neutralised, breaking the salt bridge and leading to a downward movement of Arg82.[18] The Arg movement induces a change in the second hydration shell of the protonated water cluster[5,20] and affects the water positions (Figure 5). As a consequence, the proton is shifted more towards Glu194 and 204, leading to a transient protonation. This destabilizes the hydrogen bond to Ser193, leading either to an elongation or a breaking of the bond. Consequently the proton release site opens up in M and N state and the proton is released to the bulk water.

Figure 9 furthermore indicates the influence of pH and mutation of Ser193 on this mechanism. Removal of the hydrogen bond by mutation of Ser193 in the S193A and S193C mutants increases the barrier between the protonated water cluster and bulk water. Therefore, the proton cannot leave the protein in the usual way but is pushed onto the glutamates 194 and/or 204. At higher H^+ concentrations (pH 5), this mechanism is slow enough to appear in the IR spectra of WT bR, too. This is probably due to a lowering of the difference in proton potential between water cluster and bulk water.

Conclusions

Our experimental and theoretical findings show that the hydrogen bond between Ser193 and Glu204 is crucial for an efficient and controlled proton exit in the photocycle of bR. In the ground state, the hydrogen bond closes the exit site and shields it from bulk solvent. Upon charge transfer from the

protein interior, the bond is broken, and the exit site opens up, irreversibly releasing the proton to the bulk solvent. The protein therefore actively regulates the properties of the internal protonated water network to ensure the directionality of proton transfer. The transient protonation of Glu194/204 is the key step for gate opening and proton release.

Experimental Section

Mutants and Protein: The mutagenesis and expression of bacteriorhodopsin in *Halobacterium salinarum* is described elsewhere,[21,22] as is its isolation and purification in purple membrane sheets.[23]
Sample Preparation: A suspension of 600 μg of pure membrane sheets in 1 M KCl, 100 mM Tris at pH 7 was centrifuged for 2 h at 200,000 g and the obtained pellet was squeezed between two 2 mm CaF_2 windows.
Fourier Transform Infrared (FTIR) Spectroscopy: The time-resolved data was obtained by performing Step-Scan FTIR Spectroscopy on the sample with a modified Bruker IFS66v spectrometer as previously described.[24] The sample was strictly kept at 20 °C during the whole measurement to ensure stability. The laser pulse to start the photocycle was generated by an Excimer-Laser (Lambda 305i) driven Dye-Laser based on Coumarin153.

Molecular Dynamics (MD) simulations: The inital bR structure was the 1.9 Å wild type structure of Belrhali et al. (PDB ID 1QHJ).[25] *N*-terminal amino acids 1 to 4 and side chains missing in the crystal structure were added with PyMOL.[26] The structure was checked with the MOBY program package.[27] Standard protonation states were assumed for all amino acids, except Asp96 and Asp115, which were protonated.[14] As Mathias et al. showed a preference of the proton for a specific water molecule in the proton release group,[13] water molecule HOH408 in 1QHJ was transformed into a H_3O^+ ion to mimic the proton in the exit site by means of a molecular mechanics simulation. This model for a protonated water cluster is in accordance with Garczarek et al.[5] and Mathias et al.[13]. Retinal parameters were taken from Kandt et al.[14] The resulting model was placed into a pre-equillibrated POPC bilayer surrounded by a 1 M NaCl solution in accordance with Kandt et al.[14]
Simulations were carried out with GROMACS v3.3, merging the GROMOS96 force field and lipid parameters of Berger et al.[28] in accordance with Schlegel et al.[29]. The simulation parameters and protocol were based on Wolf et al.[30] with a step size of 1 fs and no bond constraints. After protein/membrane equilibration, 20 ns of unrestrained MD simulation were performed at 293.15 K. The equilibration of the bR structure was judged by observation of the root mean square displacement of the heptahelical C_α atoms (C_α-RMSD, see Supporting Information). While the wild type protein reached a stable value of 1.6 Å after 12 ns, the S193-A mutant needed 15 ns to reach a stable C_α-RMSD of 1.0 Å. S193C already exhibits a stable C_α-RMSD of 1.1 Å after 7 ns, but shows a slight increase at the end of the simulation. Therefore, in all simulations, the final 5 ns were used for subsequent water density analysis. Water densities were calculated by the method of Kandt et al.[14] The data shown is the Connolly surface on voxels with a minimum water density of 0.1 $H_2O\,Å^{-3}$.

Acknowledgements

The authors would like to thank J. Schlitter and E. Hofmann for helpful discussions, and the NIC Jülich (Project No. hbo26) and the RRZK Köln for providing computing time. They are grateful to Gabi Smuda for the preparation of bR mutants. This work was supported by the Deutsche Forschungsgemeinschaft and by the Ruhr-University Research School funded by Germany's Excellence Initiative [DFG GSC 98/1]. All molecular representations were prepared with PyMOL.[26]

Keywords: IR spectroscopy · membrane proteins · molecular dynamics · proton transport · water chemistry

[1] C. J. T. de Grotthuss, *Ann. Chim.* **1806**, *58*, 54–74.
[2] M. Eigen, *Angew. Chem.* **1963**, *75*, 489–508; *Angew. Chem. Int. Ed.* **1964**, *3*, 1–19.
[3] Y. Hatefi, *Annu. Rev. Biochem.* **1985**, *54*, 1015–1069.
[4] A. Remy, K. Gerwert, *Nat. Struct. Bio.* **2003**, *10*, 637–644.
[5] F. Garczarek, K. Gerwert, *Nature* **2006**, *439*, 109–112.
[6] S. Hermes, J. M. Stachnik, D. Onidas, A. Rémy, E. Hofmann, K. Gerwert, *Biochemistry* **2006**, *45*, 13741–13749.
[7] B. Schobert, L. S. Brown, J. K. Lanyi, *J. Mol. Biol.* **2003**, *330*, 553–570.
[8] a) C. R. D. Lancaster, H. Michel, *Structure* **1997**, *5*, 1339–1359; b) C. R. Lancaster, M. V. Bibikova, P. Sabatino, D. Oesterhelt, H. Michel, *J. Biol. Chem.* **2000**, *275*, 39364–39368.
[9] F. Garczarek, L. S. Brown, J. K. Lanyi, K. Gerwert, *Proc. Natl. Acad. Sci. USA* **2005**, *102*, 3633–3638.
[10] J. K. Lanyi, B. Schobert, *J. Mol. Biol.* **2002**, *321*, 727–737.
[11] H. Luecke, B. Schobert, H. T. Richter, J. P. Cartailler, J. K. Lanyi, *J. Mol. Biol.* **1999**, *291*, 899–911.
[12] F. Garczarek, J. Wang, M. A. El-Sayed, K. Gerwert, *Biophys. J.* **2004**, *87*, 2676–2682.
[13] G. Mathias, D. Marx, *Proc. Natl. Acad. Sci. USA* **2007**, *104*, 6980–6985.
[14] a) C. Kandt, J. Schlitter, K. Gerwert, *Biophys. J.* **2004**, *86*, 705–717; b) C. Kandt, K. Gerwert, J. Schlitter, *Proteins* **2005**, *58*, 528–537.
[15] G. Souvignier, K. Gerwert, *Biophys. J.* **1992**, *63*, 1393–1405.
[16] H. Luecke, B. Schobert, J. P. Cartailler, H. T. Richter, A. Rosengarth, R. Needleman, J. K. Lanyi, *J. Mol. Biol.* **2000**, *300*, 1237–1255.
[17] L. Zimáni, G. Váró, M. Chang, R. Ni, R. Neeldeman, J. K. Lanyi, *Biochemistry* **1992**, *31*, 8535–8543.
[18] D. Bashford, K. Gerwert, *J. Mol. Biol.* **1992**, *224*, 473–486.
[19] V. A. Lórenz-Fonfría, Y. Furutani, H. Kandori, *Biochemistry* **2008**, *47*, 4071–4081.
[20] N. Agmon, *Chem. Phys. Lett.* **1995**, *244*, 456–462.
[21] E. Fernando, U. Schweiger, D. Oesterhelt, *Gene* **1993**, *125*, 41–47.
[22] R. Needleman, M. Chang, B. Ni, G. Varo, J. Formes, S. H. White, J. K. Lanyi, *J. Biol. Chem.* **1991**, *266*, 11 478–11 484.
[23] D. Oesterhelt, W. Stoeckenius, *Methods Enzymol.* **1974**, *31*, 667–678.
[24] R. Rammelsberg, B. Hessling, H. Chorongiewski, *Appl. Spectrosc.* **1997**, *51*, 558–562.
[25] H. Belrhali, P. Nollert, A. Royant, C. Menzel, J. P. Rosenbusch, E. M. Landau, E. Pebay-Peyroula, *Struct. Fold. Des.* **1999**, *7*, 909–917.
[26] W. L. DeLano (DeLano Scientific), Palo Alto (USA), **2002**.
[27] U. Höweler (CHEOPS), Altenberge (Germany), **2007**.
[28] a) O. Berger, O. Edholm, F. Jahnig, *Biophys. J.* **1997**, *72*, 2002–2013; b) D. P. Tieleman, M. S. P. Sansom, H. J. C. Berendsen, *Biophys. J.* **1999**, *76*, 40–49.
[29] B. Schlegel, W. Sippl, H. D. Höltje, *J. Mol. Model.* **2005**, *12*, 49–64.
[30] S. Wolf, M. Böckmann, U. Höweler, J. Schlitter, K. Gerwert, *FEBS Lett.* **2008**, *582*, 3335–3342.

Received: October 25, 2008

